Mon. Not. R. Astron. Soc. **000**, 1–13 (2010) Printed 28 April 2010 (MN LATEX style file v2.2)

Episodic Accretion on to Strongly Magnetic Stars

Caroline R. D'Angelo[1] and Hendrik C. Spruit[1]
[1] *Max Planck Institute for Astrophysics, Garching, Germany*

Accepted 20. Received ; in original form

ABSTRACT
Some accreting neutron stars and young stars show unexplained episodic flares in the form of quasi-periodic oscillations or recurrent outbursts. In a series of two papers we present new work on an instability that can lead to episodic outbursts when the accretion disc is truncated by the star's strong magnetic field close to the corotation radius (where the Keplerian frequency matches the star's rotational frequency). In this paper we outline the physics of the instability and use a simple parameterization of the disc-field interaction to explore the instability numerically, which we show can lead to repeated bursts of accretion as well as steady-state solutions, as first suggested by Sunyaev and Shakura. The cycle time of these bursts increases with decreasing accretion rate. These solutions show that the usually assumed 'propeller' state, in which mass is ejected from the system, need not occur even at very low accretion rates.

Key words: accretion, accretion discs – instabilities – MHD – stars: oscillations – stars: magnetic fields

1 INTRODUCTION

The interaction between a strong stellar magnetic field and an accretion disc can affect both the evolution and observational properties of the star. Close to the star the field is strong enough that the accretion disc is truncated, and mass is channelled along field lines to accrete on to the star's surface. At the inner edge of the truncated disc, the field and disc interact directly over some finite region, allowing angular momentum exchange from the differential rotation between the Keplerian accretion disc and the star.

Angular momentum exchange between the field and the disc leads to two different states that can exist for a disc truncated by a magnetic field. The distinction depends on the position of the truncation radius relative to the corotation radius, $r_{\rm c} \equiv (GM_*/\Omega_*^2)^{1/3}$ (where M_* and Ω_* are respectively the mass and spin frequency of the star), the radius at which the Keplerian frequency in the disc equals the star's rotational frequency. If the disc is truncated inside $r_{\rm c}$ then the field-disc interaction extracts angular momentum from the disc and accretion can proceed. If on the other hand the disc is truncated outside $r_{\rm c}$, the star-field interaction will create a centrifugal barrier that inhibits accretion. This is usually called the 'propeller regime', under the assumption that most of the mass in the disc is expelled as an outflow (Illarionov & Sunyaev 1975).

Accreting stars with strong magnetic fields such as T Tauri stars, and X-ray millisecond pulsars show a large degree of variability in luminosity (corresponding to changes in accretion rate), which may be ascribable to magnetic activity. For example, the protostar EX Lupi (the prototype of the 'EXor' class), a TTauri star, increases and decreases in brightness by several magnitudes every 2–3 years (Herbig 2007). At much higher energies, a 1 Hz quasi-periodic oscillation (QPO) in accreting millisecond pulsar SAX J1808.8-3658 has been observed during the decay phase of several outbursts (Patruno et al. 2009). The time-scale and magnitude of the variability in both sources suggest changes in accretion rate in the inner regions of the accretion disc, where it interacts with the star's magnetic field.

In this paper we revisit a disc instability first suggested in Sunyaev & Shakura (1977) and developed in Spruit & Taam (1993) (hereafter ST93), which can lead to episodic bursts of accretion. The instability arises when the magnetic field truncates the disc near the corotation radius. The magnetic field initially truncates the disc outside but close to the corotation radius, thus transferring angular momentum from the star to the disc and inhibiting gas from accreting on to the star (the propeller state). However, close to $r_{\rm c}$, the energy and angular momentum transferred by the field to the gas will not be enough to unbind much of the disc mass from the system and drive an outflow. Instead, the interaction with the magnetic field will prevent accretion (Sunyaev & Shakura 1977). As gas in the inner regions of the disc piles up, the local gas pressure increases, forcing the inner edge of the disc to move inwards until it crosses $r_{\rm c}$. When the inner region of the disc cross inside $r_{\rm c}$, the centrifugal barrier preventing accretion disappears (since now the differential rotation between star and disc has changed sign) and the accumulated reservoir of gas is accreted on to the star. Once the reservoir has been accreted, the accretion rate through the disc's inner edge decreases, and the disc will again move outside $r_{\rm c}$, allowing another cycle to start.

We study this process by following the time evolution of a thin axisymmetric viscous disc, with a paramaterization of the interaction between the disc and the magnetic field both inside and outside $r_{\rm c}$. This approach allows us to investigate the behaviour of the disc on time-scales much longer than the rotation period of the

star. Long time-scales are important since the instability evolves on viscous rather than dynamical time-scales of the disc. We are able to reduce the uncertainties in the detailed MHD interaction between the field and the disc to two free (but constrained) parameters. Using this description we can then investigate the physical conditions for which the instability develops.

In this paper we describe in detail the physics that can lead to episodic bursts of accretion and give a brief overview of the observed oscillations. In a later paper we will explore the range of outbursts seen in our simulations in more detail, and discuss their prospects for observability in specific stellar systems.

2 MAGNETOSPHERE-DISC INTERACTIONS

2.1 Interaction region between a disc and magnetic field

We consider a star with a strong dipolar magnetic field surrounded by a thin Keplerian accretion disc. We assume that the dipole is aligned with both the star's spin axis and the spin axis of the disc, so that the system is axisymmetric. Near the surface of the star the magnetic field will truncate the disc, forcing gas into corotation with the star. This inner region (in which the gas dynamics is regulated by the magnetic field) is called the magnetosphere, and we define the *magnetospheric radius*, $r_{\rm m}$ as the radius at which the magnetic field is no longer strong enough to force the disc into corotation (Spruit & Taam 1993). Outside $r_{\rm m}$ the magnetic field will penetrate the disc and become strongly coupled over some radial extent, which we call the *interaction region*, Δr. Beyond the interaction region the disc and magnetic field are decoupled, so that the outer parts of the disc are not directly affected by the stellar magnetic field. Figure 1 shows a schematic picture for the magnetic field configuration, with a closed magnetosphere close to the star, and a large region of opened field lines further out.

In the interaction region, the differential rotation between the Keplerian disc and star shears the magnetic field, generating an azimuthal component B_ϕ from the initially poloidal field. This in turn creates a magnetic stress which exerts a torque on the disc, transferring angular momentum between the disc and star. The torque per unit area exerted by the field on the disc is given by $d\mathbf{t}au/{\rm d}r = rS_{z\phi}\hat{\mathbf{z}}$, where

$$S_{z\phi} \equiv \pm\frac{B_\phi B_z}{4\pi} \quad (1)$$

is the magnetic stress generated by the twisted field lines. The sign of the torque will depend on the location of the coupled disc region relative to the corotation radius, $r_{\rm c} \equiv (GM_*/\Omega_*^2)^{1/3}$. If the coupling takes place inside $r_{\rm c}$ the torque will extract angular momentum from the disc, spinning down the disc (and spinning up the star), while if the coupling is outside $r_{\rm c}$ the torque adds angular momentum to the disc, spinning it up (and spinning down the star).

The radial extent of the interaction region has been a point of long-standing controversy in the study of accretion discs. In an early series of influential papers, Ghosh et al. (1977; Ghosh & Lamb 1979a,b) argued that the coupled region is large ($\Delta r/r \gg 1$), so that the magnetic field exerts a torque over a considerable fraction of the disc with a resulting large influence on the spin evolution of the star. However, the original model proposed by Ghosh & Lamb was shown to be inconsistent by Wang (1987), since the magnetic pressure they derived from field winding far from $r_{\rm c}$ is high enough to completely disrupt the majority of the disc.

More recent analytical and numerical work has shown that the interaction region is likely much smaller, and much of the disc is disconnected from the star (see Uzdensky 2004 for a recent review). This comes about from the fact that in force-free regions (where the magnetic pressure dominates over the gas pressure) as are likely to exist above an accretion disc, field lines will tend to open up as the twisting increases (Aly 1985; Lynden-Bell & Boily 1994). As the disc and star rotate differentially, the increasing twist $\Delta\phi$ in the field line will only increase the B_ϕ component to some maximum $B_\phi \sim B_z$ before the increased magnetic pressure above the disc causes the field lines to become inflated and eventually open, severing the connection between the disc and star. Analytic studies of a sheared force-free magnetic field (Aly 1985; van Ballegooijen 1994; Uzdensky et al. 2002) have shown that the B_ϕ component will grow to a maximum twist angle $\Delta\phi \sim \pi$ before opening. The twist angle grows on the time-scale of the beat frequency $\equiv |\Omega_* - \Omega_K|^{-1}$, which is very short compared to the viscous time-scale in the disc except in a very small region around corotation.

To prevent field lines from opening, they must be able to slip through the disc faster than the rate at which the field is being wound up. The rate at which the field can move through the disc is set by the effective diffusivity, η, of the disc. Like the effective viscosity, ν, that drives the transport of angular momentum, the effective diffusivity is also assumed to be driven by turbulent processes in the disc. Recent numerical studies of MRI (Magnetorotational Instability) turbulence (believed to be responsible for angular momentum transport in at least the inner regions of accretion discs) have tried to measure η directly. In these simulations, an external magnetic field is imposed on a shearing box simulation, and the effective magnetic diffusivity is estimated as the flow becomes unstable. The results suggest that the effective diffusivity and viscosity are of similar size, that is, the effective magnetic Prandtl number, $Pr \equiv \nu/\eta$ is of order unity (Fromang & Stone 2009). Such a large magnetic Prandtl number implies that for realistic disc parameters the magnetic field will not be able to slip through the majority of the disc fast enough enough to prevent field lines from opening (Lovelace et al. 1995; Uzdensky et al. 2002). Outside this region there will still be some coupling between the disc and the star as the gas moves from Keplerian to corotating orbits, but this estimate suggests that the actual extent of coupling is small ($\Delta r/r < 1$) regardless of where the disc is truncated relative to the corotation radius.

Once the field lines are opened, there may be some reconnection across the region above the disc between open magnetic field lines (e.g. Aly & Kuijpers 1990; Goodson et al. 1997; Uzdensky et al. 2002). The effective size of the interaction region would then depend on the efficiency of reconnection, and could also then become time-dependent (although likely on time-scales of order the dynamical time, which is much shorter than the viscous evolution time-scale). The opening and reconnection of field lines has also been suggested as a possible launching mechanism for strong disc winds and a jet (e.g. Aly & Kuijpers 1990; Hayashi et al. 1996; Goodson et al. 1997). This picture of a small interaction region with some reconnection was first proposed by Lovelace et al. (1995), and has been supported by 2 and 3D simulations of accretion discs interacting with a magnetic field (e.g. Miller & Stone 1997; Goodson et al. 1997; Hayashi et al. 1996; Romanova et al. 2009).

In summary, although the extent of the interaction region is uncertain (subject to uncertainties in the effective diffusivity of magnetic field in the disc and its possible reconnection in the magnetosphere, as well as the detailed interaction between the disc and field near the magnetosphere), numerical and analytic work suggests that

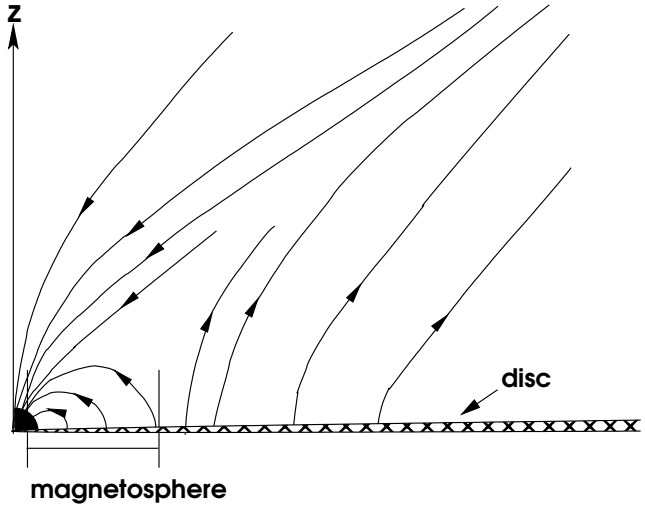

Figure 1. Global magnetic field configuration for a strongly magnetic star surrounded by an accretion disc. In this picture, the majority of the field exists in an open configuration, and the connected region between the field and the disc is very small. Adapted from Lovelace et al. (1995).

it is small. Except for very special geometries for the magnetic field (such as Agapitou & Papaloizou 2000; Shu et al. 1994), the low effective magnetic diffusivity in the disc will force the magnetic field into a largely open configuration, and the majority of the accretion disc will be decoupled from the star, in strong contrast to the prediction of the Ghosh & Lamb (1979a) model.

The extent of the interaction region as well as the average magnitude of the B_ϕ component generated by the disc-field interaction will depend on the detailed interaction between the disc and the field as the gas moves from Keplerian orbits to corotation with the star, as well as the frequency and magnitude of possible reconnection events. In the present work we therefore assume that the time-averaged B_ϕ component generated by field-line twisting will be some constant fraction of B_z, so that $B_\phi/B_z \equiv \eta < 1$. We also assume that $\Delta r/r$ is small (< 1) but leave it as a free parameter.

2.2 Accretion and angular momentum transport

In this paper we describe the evolution of an accretion disc in which the conditions at the inner boundary are changing in time. Before doing this, however, we review how the conditions at the inner boundary affect the angular momentum transport and density structure of a thin accretion disc. In the thin-disc limit the evolution equation for the surface density Σ can be written:

$$\frac{\partial \Sigma}{\partial t} = \frac{3}{r}\frac{\partial}{\partial r}[r^{1/2}\frac{\partial}{\partial r}(r^{1/2}\nu\Sigma)], \tag{2}$$

where ν is the effective viscosity in the disc that enables angular momentum transport. In a steady state (in which the accretion rate is constant throughout the disc), the general solution for $\nu\Sigma$ is given by:

$$\nu\Sigma = \frac{\dot{m}}{3\pi}\left(1 - \beta\left(\frac{r_i}{r}\right)^{1/2}\right), \tag{3}$$

where r_i is the inner edge of the disc, $\dot{m}$is the accretion rate and β is a dimensionless measure of the angular momentum flux through the disc per unit mass accreted (Popham & Narayan 1991; Paczynski 1991).

All accretion discs have a boundary layer at their inner edge that connects the disc with either the surface of the star or the star's magnetosphere. In the boundary layer the gas must transition from Keplerian orbits to orbits corotating with the star in order to accrete. The structure of this boundary layer will determine the value of β in (3). In the standard accretion scenario, that is, for accretion on to a slowly-rotating star or on to the star's magnetosphere inside the corotation radius, the gas in the boundary layer will be decelerated, meaning that there will be a maximum in the rotation profile, $\Omega(r)$. At the maximum in $\Omega(r)$, there is no longer an outward transfer of angular momentum from viscous torques, which in the thin-disc approximation will cause the surface density to decrease sharply, so that β = 1 in (3) (Pringle & Rees 1972; Shakura & Sunyaev 1973). The maximum in $\Omega(r)$ effectively corresponds to the inner radius of the disc, since inside this radius gas is viscously decoupled from the rest of disc. The gas falling through the inner boundary of the disc will add its specific angular momentum ($\dot{m}r_{\rm in}^2\Omega$) to the star, spinning it up.

However, there are in fact a wide range of solutions for the surface density profile of an accretion disc depending on the conditions imposed by the boundary layer, which in turn set the rate of angular momentum transport across the inner boundary of the disc. In a nonmagnetic star spinning close to breakup (Paczynski 1991; Popham & Narayan 1991), the angular momentum flux can be inward or outward, depending on the accretion history of the star. The dimensionless angular momentum flux β can in principle have any value less than 1 in this case. The top panel of Fig. 2 shows the steady-state surface density profile for a range of different values of β from -1 to 1.

Sunyaev & Shakura (1977) studied a similar situation in which there is outward angular momentum transport in an accretion disc, and showed adding angular momentum at the inner edge of the accretion can in fact halt accretion altogether. The evolution of the disc in this case depends on the rate at which angular momentum is being injected at the inner edge of the disc compared to the rate at which it is carried outwards via viscous coupling. If angular momentum is injected into the inner boundary of the disc at exactly the same rate as viscous transport carries it outwards, then all accretion on to the star will cease. For a steady state like this to exist, the outward angular momentum flux due to the magnetic torque at the inner edge of the disc has to be taken up at some larger distance. In a binary system, this sink of angular momentum can be the orbit of the companion star. If the disc is sufficiently large, the angular momentum can also be taken up by the outer parts of the disc, while the inner parts of the disc are close to a steady state. The inner edge of the disc then slowly moves outward under the influence of the angular momentum flux. The surface density distribution in this case can be found from (3) by taking the limit $\dot{m} \to 0$, while letting $\beta \to -\infty$ (noting that it measures the angular flux per unit accreted mass). This yields:

$$\nu\Sigma = f(r_i)\left(\frac{r_i}{r}\right)^{1/2}, \tag{4}$$

where $f(r_{\rm i})$ is a measure of the torque exterted at the inner edge of the disc. The bottom panel of Fig. 2 shows the surface density, scaled to the value of $f(r_{\rm i})$, for two instances of (4) with different values of $r_{\rm in}$.

Sunyaev & Shakura (1977) refer to this solution as a 'dead disc', since there is no accretion on to the star. In this paper we call non-accreting discs without large outflows 'quiescent discs', to avoid confusion with 'dead zones' thought to be present in protostellar discs (regions in which there is insufficient ionization to

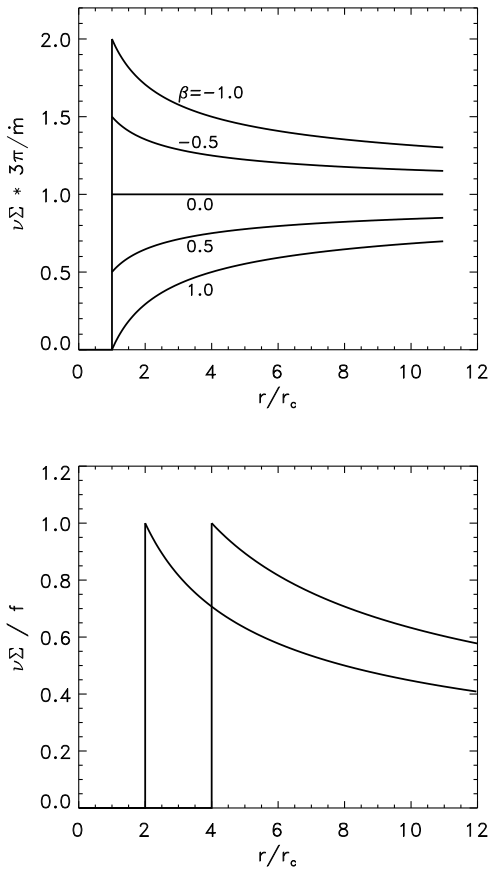

Figure 2. Surface density $\nu\Sigma$ of a thin disc as a function of distance from the corotation radius $r_{\rm c}$, for a steady, thin viscous disc. Top: steady accretion at a fixed accretion rate $\dot{m}$, for inner edge of the disc at corotation. β measures the angular momentum flux, $\beta = 1$ corresponding to the standard case of accertion on to a slowly rotation object. For $\beta < 0$ the angular mometum flux is outward (spindown of the star). Bottom: 'quiescent disc' solutions with $\dot{m} = 0$ and a steady outward angular momentum flux due to a torque f applied at the inner edge. The two curves show solutions for $r_{\rm in}/r_{\rm c} = 2$ and 4.

drive angular momentum transport via MRI but are too hot for efficient angular momentum transport via gravitational instabilities; e.g. Gammie 1996). These quiescent discs play a role in the cyclic solutions discussed in Section 3. In these solutions accreting phases are separated by long intervals in which the inner disc is close to the quiescent state described by (4).

2.3 Evolution of a disc truncated inside the corotation radius

When the accretion disc is truncated by a magnetic field inside the corotation radius, the standard $\beta = 1$ case applies for a steady-state solution. The location of the inner edge of the disc $r_{\rm in}$will be determined by the interaction between the disc and magnetic field, and change with changing conditions at the inner edge (such as the accretion rate on to the star). Here we estimate the location of $r_{\rm in}$, and use it to show how the inner boundary of the disc will change in a non-steady disc.

We define the inner edge of the disc as the point at which material in the disc is forced into corotation with the star. We use the azimuthal equation of motion for gas at the magnetospheric radius to obtain an estimate for $r_{\rm in}$in a disc (see, e.g. ST93):

$$2\pi\Sigma\frac{\partial}{\partial t}(rv_\phi) - \frac{\dot{m}_{\rm in}}{r}\frac{\partial}{\partial r}(rv_\phi) + 2\pi r S_{z\phi} = 0, \tag{5}$$

where $\dot{m}_{\rm in} = -2\pi r\Sigma v_r$ is the accretion rate through the inner edge of the disc. (5) neglects viscous angular momentum transport through the inner regions of the disc, under the assumption that it will be much smaller than angular momentum transport from the magnetic field. Using $v_\phi = \Omega_* r$ (since at $r_{\rm in}$ the gas corotates with the star), and assuming a steady-state solution ($\partial/\partial t = 0$), (5) becomes:

$$\frac{\dot{m}\Omega_*}{\pi} = r_{\rm in}S_{z\phi} = \frac{r_{\rm in}B_\phi B_z}{4\pi}, \tag{6}$$

where $S_{z\phi}$ is the magnetic stress from the coupling between the disc and star (introduced in Section 2.1). As long as the wind-up time for the field is shorter than the rate at which $r_{\rm in}$ is changing, B_ϕ/B_z will be roughly constant, so we make the assumption that $B_\phi = \eta B_z$, where $\eta < 1$ and is constant.

For a dipole field aligned with the star's axis of rotation ($B_z = \mu/r^3$, where $\mu = B_S R_*^3$ is the star's magnetic dipole moment), (6) can be re-written:

$$r_{\rm in} = \left(\frac{\eta\mu^2}{4\Omega_*\dot{m}_{\rm in}}\right)^{1/5}. \tag{7}$$

For $\eta = 0.1$, this estimate gives a value for $r_{\rm in}$ about 40% smaller than the simple estimate found by equating the magnetic pressure from the field ($B^2/8\pi$) to the ram pressure from spherically-symmetric gas in free-fall on to the star (e.g. Pringle & Rees (1972)).

The derivation for $r_{\rm in}$ above holds for steady accretion. For the problem studied here the position of the inner edge (set by the location of the magnetosphere) will change in time, which requires a minor reinterpretation of (7). If $r_{\rm in}$ is moving in time, the mass flux $\dot{m}_{\rm co}$ in the reference frame comoving with $r_{\rm in}$ differs from the mass flux, $\dot{m}$, measured in a fixed frame:

$$\dot{m}_{\rm co} = \dot{m} + 2\pi r\Sigma\dot{r}_{\rm in}, \tag{8}$$

where $\dot{r}_{\rm in}$ is the time derivative of $r_{\rm in}$.

Since the torque between the magnetosphere and the disc acts at the inner edge, the mass flux entering the magnetosphere (used in (7)) is given by $\dot{m}_{\rm co}$, not $\dot{m}$. As before, $\dot{m}$ itself is given in terms of the surface density by the usual thin disc expression:

$$\dot{m} = 3r_{\rm in}^{1/2}\frac{\partial}{\partial r}\left(r^{1/2}\nu\Sigma\right)\Big|_{r_{\rm in}}. \tag{9}$$

2.4 Evolution of a disc truncated outside the corotation radius

If the star is spinning fast enough, the magnetic field can truncate the disc *outside* $r_{\rm c}$. In this case the interaction with the magnetic field will *add* angular momentum to the disc, creating a centrifugal barrier that inhibits accretion. This scenario was first described by Illarionov & Sunyaev (1975) and is often termed the 'propeller' regime, under the assumption that the interaction with the magnetic field will expel the disc at $r_{\rm in}$ as an outflow via the 'magnetic slingshot' mechanism (Blandford & Payne 1982).

However, in order for the gas to be ejected from the system, it must be accelerated to at least the escape speed ($v_{esc} = \sqrt{GM_*/2r}$). At the inner edge of the interaction region the gas is brought into corotation with the star, where $v_{\rm c} = \Omega_* r$. If this is

less than the escape speed, the majority of the gas will not be accelerated enough to be expelled. Setting $v_{esc} = v_c = \sqrt{GM_*/r_c^3}r$ implies that for $r_{\rm in} < 1.26r_c$ most of the gas will not be expelled.

Part of the disc could still be expelled in an outflow, but while the majority of the gas remains confined in the disc, the disc can act as an efficient sink for angular momentum from the star and accretion can effectively be halted. The open field lines at larger radii could launch a disc wind which would provide an additional sink for angular momentum and somewhat change the structure of the disc (e.g. Matt & Pudritz 2005). Numerical studies of the field-disc interaction, for example, find that reconnection across field lines can lead to intermittent accretion (e.g. Goodson et al. 1997, see also Section 6). However, models of disc winds typically include mass loss rate as a parameter of the problem, so that the amount of mass actually lost to the wind is uncertain. In this paper we make the assumption that the disc becomes quiescent, that is, for $r_{\rm in} > r_c$ no accretion or outflows occur. The steady-state disc solution is then given by (4).

In the next section we will derive $f(r_{\rm in})$, the boundary condition for the surface density at the inner edge of a quiescent disc. Like for cases when $r_{\rm in} < r_c$, we want to study non-steady-state solutions in which $r_{\rm in}$ moves in time. As in the steady-state case, to derive $\dot{r}_{\rm in}$ we consider the difference in accretion rate at $r_{\rm in}$ in a fixed frame and in a frame comoving with $r_{\rm in}$. Since for a quiescent disc no matter is being accreted on to the star, $\dot{m}_{\rm co}$= 0, so that (8) can be written:

$$2\pi r\Sigma\dot{r}_{\rm in} = -3r_{\rm in}^{1/2}\frac{\partial}{\partial r}\left(r^{1/2}\nu\Sigma\right)\Big|_{r_{\rm in}}. \quad (10)$$

Together with (2), a viscosity prescription and condition for the outer boundary, we can use the results from this section and the previous one to study the time-dependent behaviour of an accretion disc interacting with a magnetic field.

3 CYCLIC ACCRETION

The existence of quiescent disc solutions can naturally lead to bursts of accretion. Since there is very little accretion on to the star or outflow, if mass continues to accrete from larger radii it will pile up in the inner regions in the disc until the gas pressure is high enough to overcome the centrifugal barrier from the magnetic field-disc interaction and accretion can proceed. Once the reservoir has been emptied the inner edge of the disc will move back outside the corotation radius and the reservoir will start to build up again.

In Sections 2.3 and 2.4 we showed how the inner radius of a thin viscous accretion disc will evolve inside and outside corotation. To study the time-dependent evolution of a disc, we must connect these two states as the inner edge of the disc passes through the corotation radius. We also require a description for $f(r_{\rm in})$, the inner boundary condition for the disc truncated outside r_c.

3.1 Surface density profile for $r_{\rm in} > r_c$

When the interaction region is outside r_c, the star is rotating faster than the Keplerian disc and the magnetic field lines lead the disc, adding angular momentum to the material in the inner regions. As discussed in Section 2.1, the torque per unit area exerted on the disc will be $\langle S_{\phi z}\rangle r$, so that the torque exerted across the entire interaction region (assuming it is small) is approximately:

$$\tau \simeq 4\pi\langle S_{\phi z}\rangle r_{\rm in}\Delta r\hat{\mathbf{z}}, \quad (11)$$

where the extra factor 2 comes from coupling to both sides of the disc.

As argued in the previous section, if the disc is truncated close to but outside r_c, the majority of the gas in the interaction region will not be expelled in an outflow. Instead, the angular momentum from the magnetic field is transferred outwards to the rest of the disc. We can derive a relationship between the position of and surface density at the inner edge of non-interacting disc from the conservation of angular momentum across the interaction region.

Since the interaction region is small we do not consider its density profile explicitly, focusing instead on its influence on the non-interacting disc. We therefore define $r_{\rm in}$ as the point in the disc just outside the interaction region, where there is no magnetic coupling between the disc and the star. Across the interaction region the density in the disc decreases sharply (since the gas is forced into nearly corotating orbits with the star). We make the simplifying assumption that none of the mass in the disc escapes, either into an outflow or through the magnetosphere on to the star. The inner edge of the interaction region, $r_{\rm in} - \Delta r$, is therefore defined as the point at which the surface density drops to zero.

To determine Σ at $r_{\rm in}$we consider the angular momentum flux across Δr when $r_{\rm in} > r_c$. The flux of angular momentum must be continuous across Δr, meaning that the viscous angular momentum transport outside Δr must balance the angular momentum flux added by the magnetic field across the interaction region. This balance is written:

$$\dot{m}r^2\Omega - 2\pi r(\nu\Sigma)^+r^2\Omega' = \quad (12)$$
$$\dot{m}r^2\Omega - 2\pi r(\nu\Sigma)^-r^2\Omega' + \int_{r_{\rm m}}^{r_{\rm m}+\Delta r} 4\pi r^2 S_{z\phi}dr.$$

In this equation, $\nu^{\pm}$ and $\Sigma^{\pm}$ are the viscosity and surface density inside ($^-$) and outside ($^+$) Δr, $\dot{m} = 2\pi r(\Sigma v_r)^{\pm}$ is the mass flux through Δr (where v_r is the radial velocity of the gas) and Ω is the orbital frequency at $r_{\rm in}$. The first term on either side of the equation denotes the advection of angular momentum across $r_{\rm in}$, while the second is the angular momentum transported by viscous stresses. The final term on the right hand side is the angular momentum added by the magnetic field to the coupled region of the disc. The first term on both sides cancel (to enforce conservation of mass across Δr), and we make the further assumption that in the interaction region most of the angular momentum is transported through external magnetic torques rather than viscous stress, so that $(\nu\Sigma)^- \ll (\nu\Sigma)^+$. For a small interaction region, the last term in (12) can be re-written:

$$\int_{r_{\rm in}-\Delta r}^{r_{\rm in}} 4\pi r S_{z\phi}dr \approx 4\pi\Delta r r_{\rm in}\langle S_{z\phi}\rangle. \quad (13)$$

(12) can then be re-written to yield the surface density at $r_{\rm in}$ for $r > r_c$:

$$(\nu\Sigma)^+ = -\frac{2\langle S_{z\phi}\rangle\Delta r}{\pi r_{\rm in}\Omega'}. \quad (14)$$

As predicted in Section 2.4, (14) shows that the surface density at $r_{\rm in}$ will be large, a consequence of the torque being applied by the disc-magnetic field coupling (Sunyaev & Shakura 1977; Popham & Narayan 1991; Paczynski 1991). (14) corresponds to the function $f(r_{\rm in})$ introduced in Section 2.2 for $r_{\rm in} > r_c$, that is, the boundary condition at the inner edge of the disc. In a time-dependent system, as gas accretes from larger radii (via viscous torques) it will pile up near $r_{\rm in}$and the increased gas pressure will push the inner edge of the disc further inwards towards r_c.

3.2 Transition region

When the inner edge $r_{\rm in}$ is well inside $r_{\rm c}$, conditions at the inner edge are the standard ones for accretion of a thin disc on a slowly rotating object:

$$\Sigma(r_{\rm in}) = 0, \tag{15}$$

while the time-dependent position of the inner edge is determined by (7):

$$r_{\rm in} = \left(\frac{\eta\mu^2}{4\Omega_* \dot{m}_{\rm co}}\right)^{1/5}, \tag{16}$$

where $\dot{m}_{\rm co}$ is the mass flux in a frame comoving with $r_{\rm in}$ as discussed above.

When the inner edge is outside the corotation radius, the magnetosphere does not accrete:

$$\dot{m}_{\rm co} = 0, \tag{17}$$

while the surface density at $r_{\rm in}$ is determined by a magnetic torque, as discussed above. With the Keplerian value for $\Omega(r_{\rm in})$ and assuming a dipolar magnetic field, the results of Section 3.1 can be re-written:

$$(\nu\Sigma)^+ = \frac{\eta\mu^2}{3\pi(GM_*)^{1/2}} \frac{\Delta r}{r_{\rm in}^{9/2}}. \tag{18}$$

To connect these two limiting cases, we assume that the effect of the interaction processes is equivalent to a smooth transition in the conditions. This is valid since the time-scales we are interested in are much longer than the orbital time-scale on which the conditions of the transition region between disc and magnetosphere vary. The assumption is thus that the effect of the fast processes in the transition region can be represented by averages. The mass flux on to the magnetosphere is therefore taken to vary smoothly from 0 for $r_{\rm in}$ well outside corotation to the value in (16) valid well inside:

$$\dot{m}_{\rm co} = y_m \dot{m}^+, \tag{19}$$

where $\dot{m}^+$ is given by (16). For the connecting function y_m we take a simple function that varies from 0 to 1 across the transition:

$$y_m = \frac{1}{2}\left[1 - \tanh\left(\frac{r_{\rm in} - r_{\rm c}}{\Delta r_2}\right)\right] \tag{20}$$

where Δr_2 is the nominal width of the disc-magnetosphere transition and a parameter of the problem.

Similarly the surface density at the inner edge makes a smooth transition from its value in (18) to 0:

$$\Sigma_{\rm in} = y_\Sigma \Sigma^+, \tag{21}$$

where the connecting function y_Σ is:

$$y_\Sigma = \frac{1}{2}\left[1 + \tanh\left(\frac{r_{\rm in} - r_{\rm c}}{\Delta r}\right)\right]. \tag{22}$$

All the uncertainties in the transition region are thus subsumed in the parameters Δr and Δr_2. In Section 5 we study the effect of these uncertainties with a parameter survey. The effective widths of the transition of magnetospheric accretion rate and inner-edge surface density need not be the same, and we in fact find that the difference between Δr and Δr_2 is important for the form of the resulting accretion cycles.

3.3 Physical constraints on Δr and Δr_2

In this paper we treat Δr and Δr_2 as free parameters. However, a lower limit on both parameters can be set by considering the stability of the inner regions of the disc to the interchange instability. In the quiescent disc, the low-density magnetosphere must support the high-density disc against infall. This configuration will be unstable to interchange instability (the analog of the Kelvin-Helmholtz instability), unless the surface density gradient in the interaction region is shallow enough to suppress it. This sets a limit on the minimum width of the interaction region, Δr, where the density gradient falls from its maximum (at $r_{\rm in}$) to close to zero in the magnetosphere.

This instability also sets a limit on the minimum width of Δr_2, the transition length over which the disc moves from a non-accreting quiescent disc to one in which there is accretion through the inner boundary. As $r_{\rm in}$ moves closer to $r_{\rm c}$ the width of the interaction region preventing accretion (i.e. where the field lines are adding angular momentum to the disc) decreases. When the width of the interaction region outside $r_{\rm c}$ becomes smaller than is stable against the interchange instability, accretion through the magnetosphere will begin. Δr_2 must therefore be larger or equal to this value, that is, at this minimum distance from $r_{\rm c}$ accretion onto the star will take place.

Spruit et al. (1995) studied the stability of a disc interacting with a magnetic field to interchange instabilities, and derived the following linear stability criterion:

$$\frac{B_r B_z}{2\pi\Sigma} \frac{\rm d}{{\rm d}r} \ln\left|\frac{\Sigma}{B_z}\right| > 2\left(r\frac{{\rm d}\Omega}{{\rm d}r}\right)^2. \tag{23}$$

Assuming that $B_r \sim B_\phi$, in our formulation this inequality becomes:

$$\frac{3\alpha}{1 + \tanh\left(\frac{\Delta r_2}{\Delta r}\right)} \left(\frac{H}{r}\right)^2 > 2\left(1 - \left(\frac{r_{\rm in}}{r_{\rm c}}\right)^{3/2}\right)^2. \tag{24}$$

For $\alpha = 0.1$ and assuming H/r is in the range 0.07–0.1, the range of $\Delta r/r = [0.05, 0.1]$ will satisfy this inequality for $\Delta r_2/r = [0.01, 0.02]$. In this inequality larger values of Δr correspond to smaller possible values for Δr_2, since larger Δr correspond to smaller maximum $\Sigma(r_{\rm in})$ and hence shallower gradients. This instability has recently been studied using 3D numerical simulations (Kulkarni & Romanova 2008), who find numerically approximately the same criterion for stability as Spruit et al. (1995). The shaded regions of Figs. 7 and 8 show the values for Δr_2 and Δr that are unstable to the instability studied in this paper. The simple analysis of this section suggests that at least part of the shaded sections in Figs. 7 and 8 will be stable against the interchange instability, so that the larger magnetosphere-disc instability could occur.

4 NUMERICAL IMPLEMENTATION

4.1 Disc equation and viscosity prescription

To study the surface density evolution of an accretion disc interacting with a magnetic field as outlined in the previous section, we use a time-dependent numerical simulation of a diffusive accretion disc. Our assumption that the interaction region is small ($\Delta r/r < 1$) means that rather than calculate the disc behaviour in the interaction region explicitly we can instead use the physics of the interaction region to derive boundary conditions for the inner edge of the non-interacting disc.

We assume that the accretion disc (outside the interaction region) can be treated in the thin-disc limit, so that the evolution equation for the surface density Σ is given by (2). We assume that the viscosity in the disc follows a power-law dependence, so that:

$$\nu = \nu_0 r^{\gamma}, \tag{25}$$

where $\nu_0 = \alpha(GM_*)^{1/2}(H/R)^2$ and $\gamma = 0.5$ following the standard α-viscosity prescription (Shakura & Sunyaev 1973). To evolve (2) in time, we require boundary conditions at $r_{\rm in}$ and $r_{\rm out}$, plus an additional equation to describe the movement of the inner edge of the disc, $\dot{r}_{\rm in}$. We set the outer boundary by defining the mass accretion rate through the outer edge of the disc ($\dot{m}$), which we vary as a parameter of the problem. This defines the time-averaged mass accretion rate in the disc. The surface density at the inner edge of the disc is given by (21):

$$\Sigma(r_{\rm in}) = \frac{\eta\mu^2}{6\pi(GM_*)^{1/2}\nu_0}\frac{\Delta r}{r_{\rm in}^{9/2+\gamma}}\left[\tanh\left(\frac{r_{\rm in}-r_{\rm c}}{\Delta r}\right)+1\right]. \tag{26}$$

We calculate the displacement of the inner boundary using the results of Sections 2.3 and 2.4, by considering the difference between the total mass flux at $r_{\rm in}$ in a fixed and comoving frame of reference:

$$\dot{m}_{\rm co} = \dot{m} + 2\pi r\Sigma\dot{r}_{\rm in}, \tag{27}$$

where $\dot{m}_{\rm co}$ is given by (19). This expression can be re-written:

$$6\pi r_{\rm in}^{1/2}\frac{\partial}{\partial t}(\nu\Sigma r_{\rm in}) = -2\pi r_{\rm in}\Sigma(r_{\rm in})\dot{r}_{\rm in} + \left[1-\tanh\left(\frac{r_{\rm in}-r_{\rm c}}{\Delta r_2}\right)\right]\frac{\eta\mu^2}{8\Omega_* r_{\rm in}^5}. \tag{28}$$

Taken together, (2), (25), (26), (28) and an outer boundary condition describe the time-dependent evolution of an accretion disc.

4.2 Steady-State solution

From the results of the previous sections, we can calculate the steady-state solutions for a given $\dot{m}$, the average mass accretion rate. For certain values of $\dot{m}$, Δr and Δr_2, this equilibrium is unstable, leading to oscillations in $r_{\rm in}$ and corresponding accretion bursts.

In a steady-state, the accretion rate is constant throughout the disc, i.e. $\dot{m}_{\rm co} = \dot{m}$:

$$\dot{m} = \frac{1}{2}\left[1-\tanh\left(\frac{r_{\rm in}-r_{\rm c}}{\Delta r_2}\right)\right]\frac{\eta\mu^2}{4\Omega r_{\rm in}^5}. \tag{29}$$

Implicitly solving (29) for $r_{\rm in}$ yields the inner radius of the disc in a steady-state solution.

The general steady-state surface density profile was calculated in Section 2.2, and is given by (4) with an additional term since $\dot{m} \neq 0$ in the disc. The function $f(r_{\rm in})$ is given by equation (18). The steady-state surface density profile will thus be:

$$\nu\Sigma = \frac{\dot{m}}{3\pi}\left[1-\left(\frac{r_{\rm in}}{r}\right)^{1/2}\right] + \frac{\eta\mu^2\Delta r}{6\pi r_{\rm in}^4(GMr)^{1/2}}\left[1+\tanh\left(\frac{r_{\rm in}-r_{\rm c}}{\Delta r}\right)\right] \tag{30}$$

The numerical simulations described in the following sections of the evolution of a viscous accretion disc show that the equilibrium solution given by (29) and (30) can become unstable to episodic bursts of accretion by the process outlined in Section 3.

4.3 Numerical setup

To follow the time-dependent evolution of a viscous accretion disc interacting with a magnetic field we use a 1D numerical simulation, first making a series of mathematical transformations.

The power-law prescription for the viscosity, (25), allows us to define a new function, u, for convenience:

$$u \equiv \Sigma r^{1/2+\gamma} \tag{31}$$

To make our results more readily applicable to different magnetic stars (e.g. neutron stars, magnetic white dwarves and protostars), we adopt scale-free coordinates. The instability studied in this paper varies on viscous time-scales of the inner disc, which are in general much shorter than the time-scale over which the transfer of angular momentum between the star and the disc can substantially change the star's rotation period. A constant rotation period implies that a constant corotation radius, making it a natural choice for scaling our variables. We thus scale the radial coordinate to the corotation radius, and the time in terms of the viscous time-scale (r^2/ν) at the corotation radius. Further, since we are most interested in the behaviour of inner regions of the disc, we adopt a coordinate system comoving with $r_{\rm in}$:

$$r' \equiv \frac{r-r_{\rm in}}{r_{\rm c}}; t' \equiv t\frac{\nu_0}{r_{\rm c}^{2-\gamma}}. \tag{32}$$

Dropping the prime notation, the surface density evolution equation in the new coordinate system then becomes:

$$\frac{\partial u}{\partial t} = 3r^{\gamma-1/2}\frac{\partial}{\partial r}\left[r^{1/2}\frac{\partial u}{\partial r}\right] + \dot{r}_{\rm in}\frac{\partial u}{\partial r}, \tag{33}$$

with the boundary condition at $r_{\rm in}$ given by:

$$u(r_{\rm in}) = \frac{\eta\mu^2}{3\pi(GM_*)^{1/2}\nu_0 r_{\rm c}^4}\frac{\Delta r}{r_{\rm in}}r_{\rm in}^{-3}\left[\tanh\left(\frac{r_{\rm in}-1}{\Delta r}\right)+1\right]. \tag{34}$$

The evolution of the inner edge of the disc is given by:

$$\dot{r}_{\rm in} = \left[1-\tanh\left(\frac{r_{\rm in}-1}{\Delta r_2}\right)\right]\frac{\eta\mu^2}{16\pi\Omega_*\nu_0^2 r_{\rm c}^{\gamma-3/2}}\frac{r_{\rm in}^{-11/2+\gamma}}{u(r_{\rm in})} - \frac{3r_{\rm in}^{\gamma}}{u(r_{\rm in})}\frac{\partial u}{\partial r}\Big|_{r_{\rm in}}. \tag{35}$$

Finally, to increase the resolution at the inner edge of the disc we make a further coordinate transformation to an exponentially scaled grid:

$$x \equiv \frac{1}{a}\left[\ln\left(\frac{r-r_{\rm in}}{r_{out}-r_{\rm in}}\right)+1\right], \tag{36}$$

where a is a scaling factor to set the clustering of grid points around $r_{\rm in}$.

We calculate the second-order discretization of the spatial derivatives on an equally-spaced grid in x. To evolve the resulting system of equations in time requires an algorithm suitable for stiff equations. This is necessary to follow the evolution of the inner boundary, (28). When $r_{\rm in} \gg r_{\rm c}$, (28) reduces to a differential equation that is first order in time. However, for $r_{\rm in} \ll r_{\rm c}$, $\Sigma(r_{in})$ becomes very small, and the equation essentially becomes time-independent. We have formulated the problem so that $\Sigma(r_{\rm in})$ stays small but non-zero for all values of $r_{\rm in}$ (so that the solutions is continuous at all values of $r_{\rm in}$), but its small value inside $r_{\rm c}$ means that the differential equation is stiff (since the evolution equation for $r_{\rm in}$ in (28) contains terms of very different sizes). To perform the time evolution, we therefore use the semi-implicit extrapolation method

(Press et al. (1992), p. 724), which is second-order accurate in time and suitable for stiff equations.

Since the grid comoves with the inner radius, the outer boundary of our disc also moves. We set the accretion rate at the outer boundary to be fixed in the moving coordinate system, so that it changes slightly as the outer boundary moves. The effect is negligible as long as the disc is large enough that the outer parts of the disc are unaffected by the changing inner boundary condition, which we confirm by varying the position of the outer boundary of the disc.

The solutions are sensitive to the changing conditions at the inner boundary of the disc. To confirm that our results are robust for the grid we have chosen, we varied the various numerical parameters of the problem: grid resolution, the exponential stretch parameter a at the inner boundary (see (36)) and the fractional accuracy of the solution computed by the semi-implicit extrapolation method (which sets the maximum possible timestep).

5 RESULTS

Our primary goal in this paper is to study the conditions for which the disc is unstable to episodic outbursts. To do this we follow the evolution of an accretion disc in which the mean mass accretion rate, $\dot{m}$ is a parameter of the problem by setting $\dot{m}$ as the accretion rate through the disc's outer boundary. The other system parameters of the problem are the stellar mass, M_*, frequency, Ω_*, and magnetic moment, μ. The interaction between the magnetic field and the disc introduces three additional parameters: $\eta \equiv B_\phi/B_z$, the fractional width of the interaction region $\Delta r/r$, and the length scale $\Delta r_2/r$ over which the inner edge of the disc moves from a non-accreting to accreting state. Finally, our description of the viscosity, (25), introduces three additional parameters: α, the aspect ratio of the disc, H/R (assumed constant), and γ, the radial power-law dependence of the viscosity.

The problem has two scale invariances, which reduces the number of free parameters. As seen in (25), α and H/R are degenerate. Additionally, the system parameters μ, M_*, Ω_* and $\dot{m}$ can be re-written as the ratio $\dot{m}/\dot{m}_{\rm c}$, where $\dot{m}_{\rm c}$ is the accretion rate in (7) that puts the magnetospheric radius at $r_{\rm c}$. This ratio is equivalent to the 'fastness parameter', $\Omega_{\rm in}/\Omega_*$ (where $\Omega_{\rm in}$ is the Keplerian frequency at $r_{\rm in}$) which is sometimes used to describe disc-magnetosphere interactions.

For reference, our dimensionless parameter $\dot{m}/\dot{m}_{\rm c}$ can be expressed in terms of physical parameters appropriate for protostellar systems:

$$\frac{\dot{m}}{\dot{m}_{\rm c}} = \left(\frac{\dot{m}}{2.3\times10^{-7}M_\odot{\rm yr}^{-1}}\right)\left(\frac{M_*}{0.6M_\odot}\right)^{5/3} \left(\frac{B_s}{2000{\rm G}}\right)^{-2}\left(\frac{R_*}{2.1R_\odot}\right)^{-6}\left(\frac{P_*}{1\ {\rm day}}\right)^{7/3}. \quad (37)$$

We assume that the time-averaged B_ϕ component will be constant with radius in the coupled region, and set the parameter $\eta = 0.1$. For the viscosity, $\nu = \alpha(GM_*)^{1/2}(H/R)^2 r^\gamma$, we take $\alpha = 0.1$ and $H/R = 0.1$ to calculate the magnitude of ν_0, and assume $\gamma = 0.5$ everywhere in the disc. Varying α, H/R and γ will change the time-scale over which outbursts occur, but will not change the general character of our outburst solutions.

This leaves three scale-free parameters in the problem: $\dot{m}/\dot{m}_{\rm c}$, $\Delta r/r$ and $\Delta r_2/r$. We vary each of these parameters to explore the range of unstable solutions. For small values of $\Delta r/r$ (~ 0.1) and $\Delta r_2/r$ (~ 0.01), and $\dot{m}/\dot{m}_{\rm c} < 1$, the position of the inner boundary quickly becomes unstable and begins oscillating. Since the position of $r_{\rm in}$ determines the mass accretion rate on to the star, (19), the change in $r_{\rm in}$ leads to an accretion outburst. We use the steady-state solution (given by (29) and (30)) as an initial condition for all our simulations.

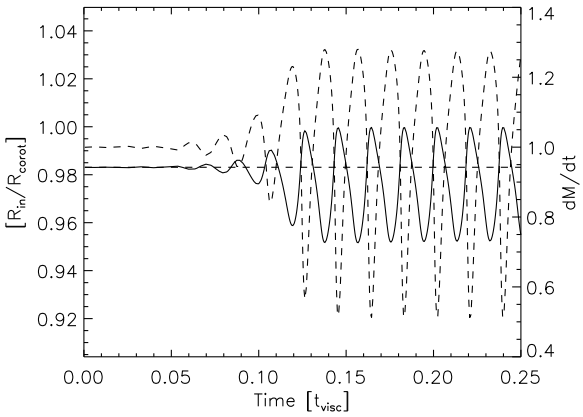

Figure 3. Growth of instability from steady-state solution, (29) and (30), for $\dot{m}/\dot{m}_{\rm c}$ = 1, $\Delta r/r = 0.05$, and $\Delta r_2/r = 0.014$. The inner radius (solid curve) evolves around its steady-state value (dashed horizontal line), causing the net accretion rate on to the star to change as well (dashed curve).

Fig. 3 shows the growth of the instability for $\dot{m}/\dot{m}_{\rm c}$ = 1, $\Delta r/r = 0.05$ and $\Delta r_2/r = 0.014$. The solid curve shows the evolution in $r_{\rm in}$, scaled to the corotation radius. The horizontal dashed line shows the steady-state value for $r_{\rm in}$. The right-hand axis plots the accretion rate on to the star as a function of time (the dashed curve). The accretion rate is scaled to units of the steady-state accretion rate, $\dot{m}$. The instability quickly grows out of the equilibrium solution, and saturates into steady oscillations.

We observe a wide range of oscillatory solutions that span three orders of magnitude in frequency, depending on the values of $\dot{m}/\dot{m}_{\rm c}$, $\Delta r/r$ and $\Delta r_2/r$. The shape of the accretion burst itself also changes dramatically depending on the system parameters. At large $\dot{m}/\dot{m}_{\rm c}$ the bursts are quasi-sinusoidal oscillations, as in Fig. 3 and the bottom panel of Fig. 4. As the mean accretion rate is decreased, the bursts take the shape of a relaxation oscillator, where the bursts are characterized by an initial sharp spike of accretion which then relaxes to a quasi-steady accretion rate for the duration of the burst, before abruptly turning off as the reservoir is emptied and $r_{\rm in}$ quickly moves well outside $r_{\rm c}$. During the outburst phase, higher frequency sub-oscillations are also sometimes seen with varying intensity.

Figs. 4 and 5 show the evolution of $r_{\rm in}$ and accretion rate as we vary $\dot{m}/\dot{m}_{\rm c}$ but the other parameters stay fixed. From bottom to top, the panels of Fig. 4 show the instability for $\dot{m}/\dot{m}_{\rm c}$ = [0.095, 0.052, 0.031] ($\dot{m} = [2.2, 1.2, 0.73] \times 10^{-8} M_\odot{\rm yr}^{-1}$ for the parameters in (37)). At the highest mean accretion rate, $r_{\rm in}$ (the solid curve) oscillates with a high frequency around its steady-state value (dashed line), with corresponding bursts of accretion on to the star (dashed curve). As $\dot{m}/\dot{m}_{\rm c}$ is decreased, the accretion profile changes to much lower frequency outbursts, with long periods of quiescence as $r_{\rm in}$ moves away from $r_{\rm c}$ and accretion ceases completely. The high-frequency oscillation that dominates for $\dot{m}/\dot{m}_{\rm c}$ = 0.095 is superimposed over the low-

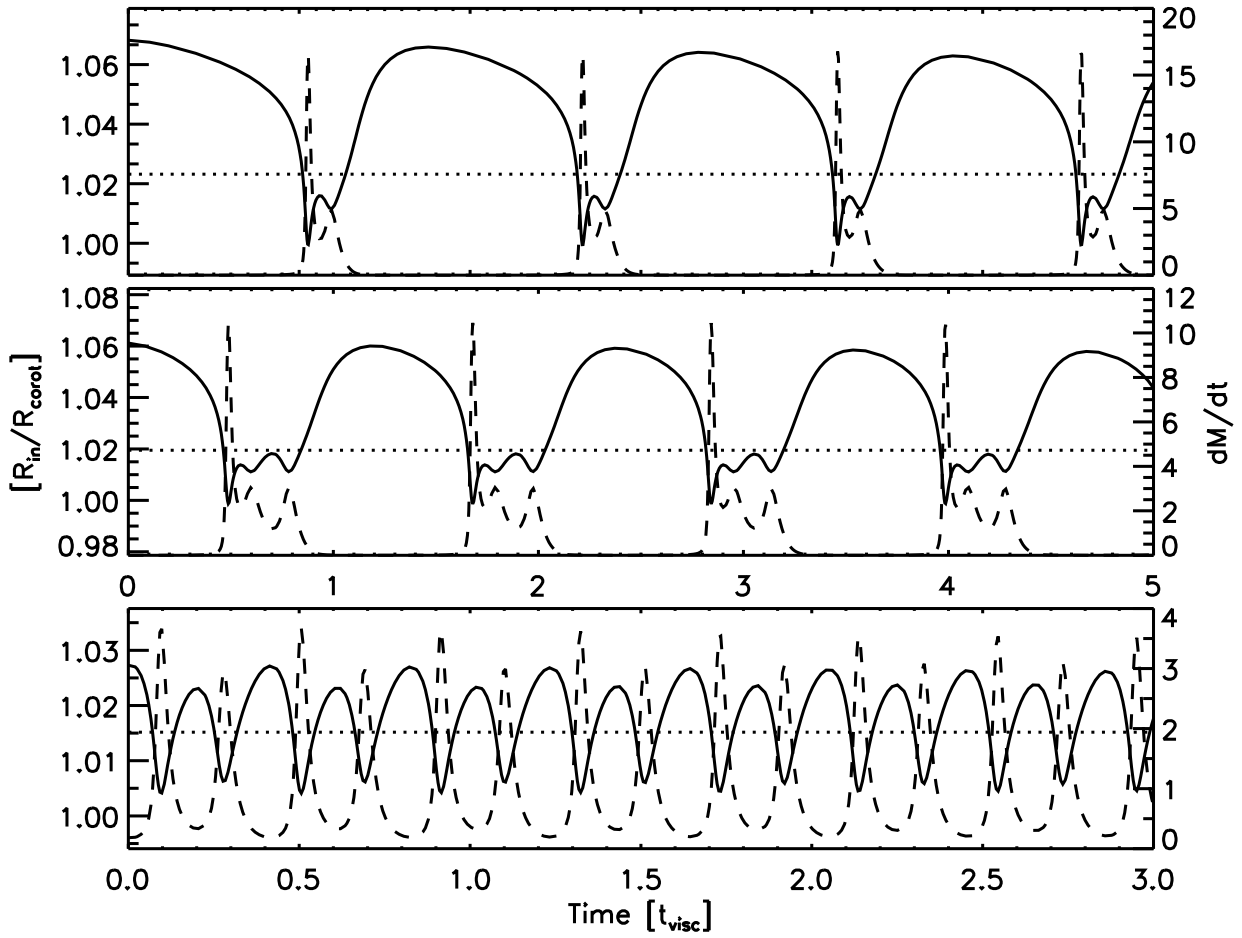

Figure 4. Outburst profiles of $r_{\rm in}$ and $\dot{m}$ for moderate values of $\dot{m}/\dot{m}_{\rm c}$. From bottom to top, $\dot{m}/\dot{m}_{\rm c}$ = [0.095,0.052, 0.031]. For adopted protostellar parameters this corresponds to $\dot{m} = [2.2, 1.2, 0.73] \times 10^{-8} M_{\odot}{\rm yr}^{-1}$. The lines are the same as in Fig. 3.

frequency accretion bursts for lower $\dot{m}/\dot{m}_{\rm c}$. Fig. 5 shows the continuation of Fig. 4 for $\dot{m}/\dot{m}_{\rm c}$ = [0.019,0.0084,0.003,0.0022] ($\dot{m} = [4.5, 1.9, 0.95, 0.38] \times 10^{-9} M_{\odot}{\rm yr}^{-1}$). The characteristic accretion burst profile essentially stays the same as $\dot{m}/\dot{m}_{\rm c}$ is decreased, with sharp spikes at the beginning and end of an accretion outburst. The overall amplitude of the outburst decreases only slightly with decreasing mean accretion rate. The initial spike decreases by about 20% as the mean accretion rate drops from $\dot{m}/\dot{m}_{\rm c}$ = 0.052 to $\dot{m}/\dot{m}_{\rm c}$ = 0.0022. The more significant effect is that the length of time between outbursts increases with decreasing $\dot{m}/\dot{m}_{\rm c}$, since at low average accretion rates it takes longer to build enough mass to drive another outburst. The overall shape of the outburst is relatively insensitive to changing $\dot{m}/\dot{m}_{\rm c}$, becoming shorter as $\dot{m}/\dot{m}_{\rm c}$ decreases. At the lowest accretion rate ($3.8 \times 10^{-10} M_{\odot}{\rm yr}^{-1}$; the top panel of Fig. 5), the burst consists of only one sharp spike. As we have formulated the problem, the instability will persist down to arbitrarily low accretion rates.

Changing the other parameters, $\Delta r/r$ and $\Delta r_2/r$, has a much stronger effect on the shape of the outburst than changing the mean accretion rate. Fig. 6 shows the outburst profiles for different values for $\Delta r/r$, setting $\dot{m}/\dot{m}_{\rm c}$ = 0.04 and $\Delta r_2/r = 0.014$. From the bottom to top, $\Delta r/r$ = [0.03,0.05,0.07,0.09], which spans the unstable region of $\Delta r/r$ for the adopted $\dot{m}/\dot{m}_{\rm c}$. For small $\Delta r/r$ the instability manifests itself as repeating short bursts of accretion, with comparatively long quiescent phases. As $\Delta r/r$ increases, the frequency of the outburst decreases, and the duty cycle increases dramatically. For very large $\Delta r/r$ the outburst lasts about 200 times as long as for the minimum $\Delta r/r$ but at lower accretion rate after the initial spike. The burst profile of the instability is thus sensitive to small changes in $\Delta r/r$, but the range in $\Delta r/r$ over which the instability exists is quite small.We find a similar range of outburst profiles by changing $\Delta r_2/r$ and keeping $\Delta r/r$ fixed, except with the opposite trend: for large $\Delta r_2/r$ the instability manifests as a series of short spiky bursts, becoming longer as $\Delta r_2/r$ decreases.

We next considered the parameter space in $\dot{m}/\dot{m}_{\rm c}$, $\Delta r/r$ and $\Delta r_2/r$ over which the instability occurs. We have briefly explored the effect of varying both $\Delta r/r$ and $\Delta r_2/r$ over a small range in $\dot{m}/\dot{m}_{\rm c}$ and found that, although the outburst profile changes somewhat, the range over which $\Delta r/r$ and $\Delta r_2/r$ produce unstable solutions are independent. We therefore assume that $\Delta r/r$ and $\Delta r_2/r$ vary independently of each other for all $\dot{m}/\dot{m}_{\rm c}$, and consider the range of the instability over the [$\dot{m}/\dot{m}_{\rm c}$, $\Delta r/r$] and [$\dot{m}/\dot{m}_{\rm c}$, $\Delta r_2/r$] spaces separately.

Fig. 7 shows the range of unstable solutions (shown as shaded regions) changing $\dot{m}/\dot{m}_{\rm c}$ and $\Delta r/r$, but keeping $\Delta r_2/r$ fixed at 0.014. Although there is a small unstable branch around $\dot{m}/\dot{m}_{\rm c}$ = 1, in general as $\Delta r/r$ increases, a lower $\dot{m}/\dot{m}_{\rm c}$ is required before the instability sets in.

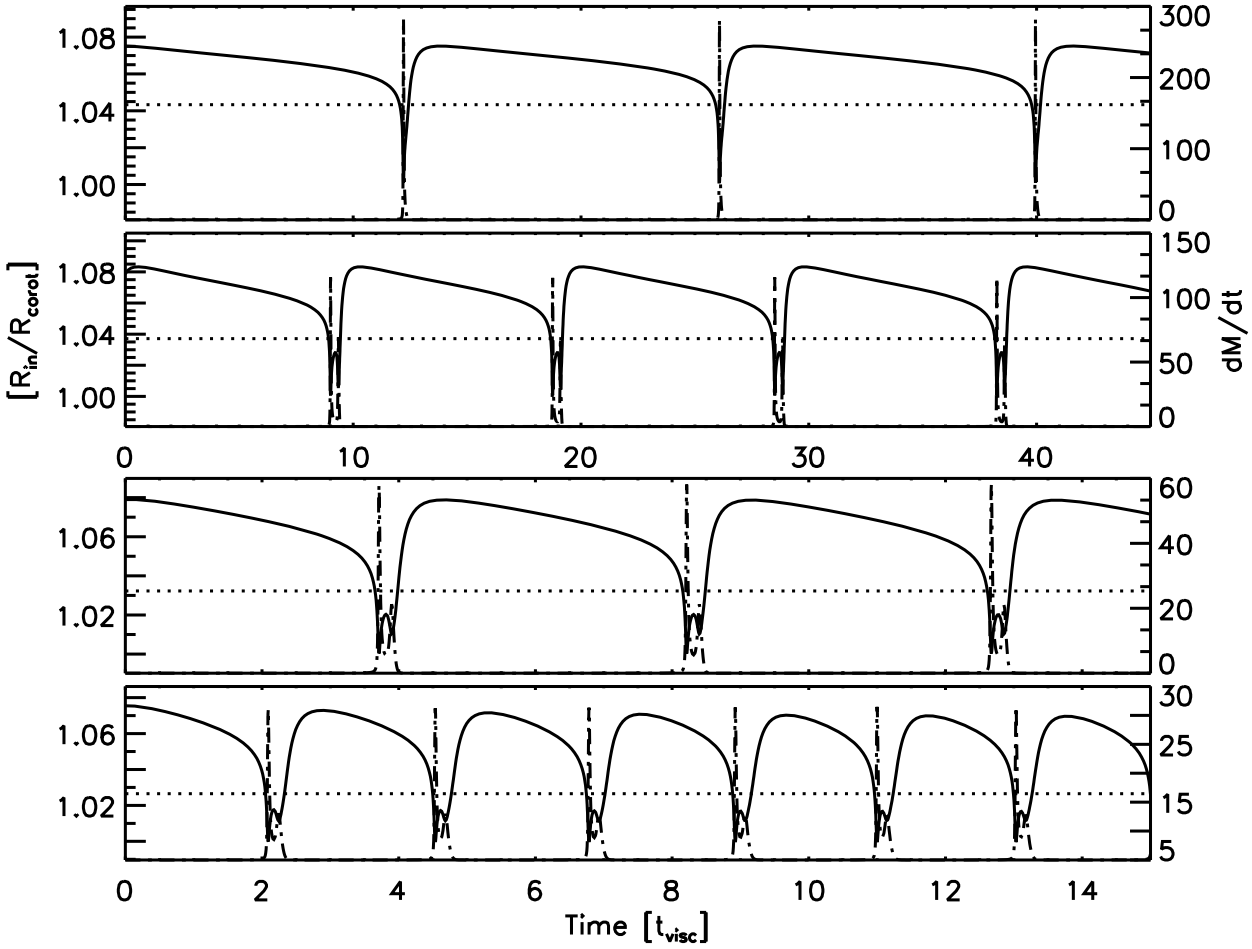

Figure 5. Outburst profiles of $r_{\rm in}$ and $\dot{m}$ for small values of $\dot{m}/\dot{m}_{\rm c}$.From bottom to top, $\dot{m}/\dot{m}_{\rm c}$ = [0.019,0.0084,0.003,0.0022]. For adopted protostellar parameters this corresponds to $\dot{m} = [4.5, 1.9, 0.95, 0.38] \times 10^{-9} M_{\odot}{\rm yr}^{-1}$. The lines are the same as in Fig. 3.

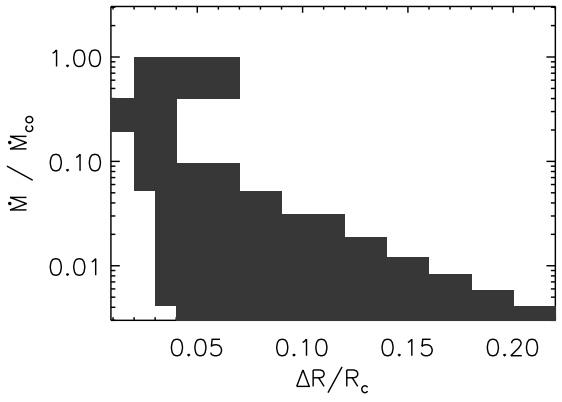

Figure 7. Parameter map of instability as a function of $\dot{m}/\dot{m}_{\rm c}$ and width of interaction region $\Delta r/r$, with constant $\Delta r_2 = 0.014$. The shaded regions denote unstable parameters.

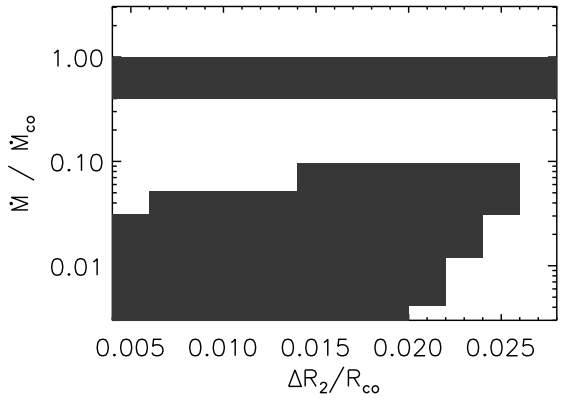

Figure 8. Parameter map of instability as a function of $\dot{m}/\dot{m}_{\rm c}$ and accretion transition length $\Delta r_2/r$, with constant $\Delta r_2 = 0.014$. The shaded regions denote unstable parameters.

Fig. 8 shows the unstable solutions changing $\dot{m}/\dot{m}_{\rm c}$ and $\Delta r_2/r$ but keeping $\Delta r/r$ fixed at 0.05. The opposite trend from Fig. 7 is seen, with a larger range of unstable accretion rates. There is again a range of unstable solutions around $\dot{m}/\dot{m}_{\rm c}$ = 1, although in this case the unstable region extends over the entire $\Delta r_2/r$ parameter space. The instability likely extends to smaller $\Delta r_2/r$, but we do not explore the region smaller than $\Delta r_2 = 0.005$ on physical grounds, since such a small transition length will likely be unsta-

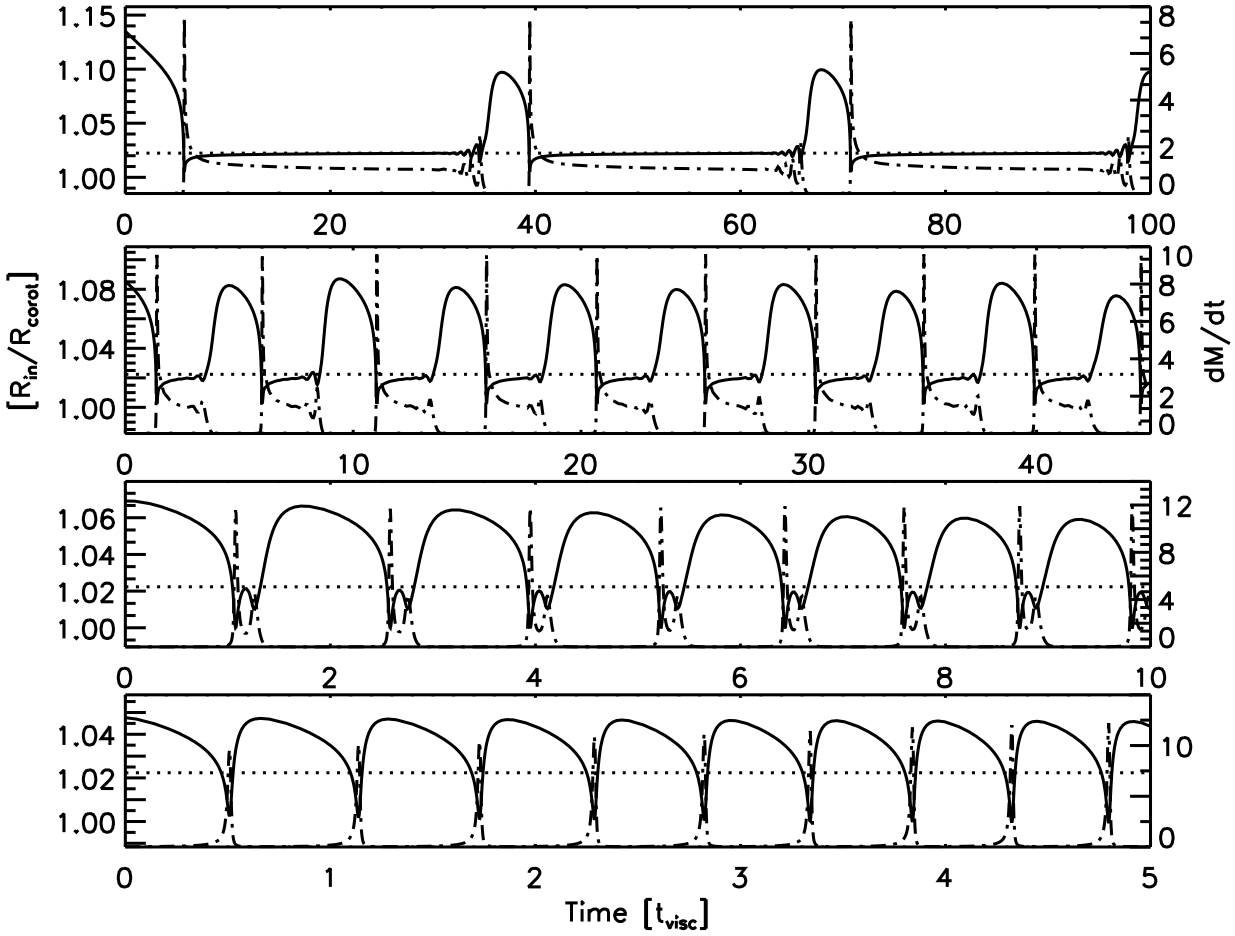

Figure 6. Outburst profiles of $r_{\rm in}$ and $\dot{m}$ for changing $\Delta r/r$, with $\Delta r_2/r = 0.014$ and $\dot{m}/\dot{m}_{\rm c}$ = 0.04. From bottom to top, $\Delta r/r = [0.03, 0.05, 0.07, 0.09]$. The lines are the same as in Fig. 3.

ble to other instabilities like the interchange instability (see Section 3.3). As with changing $\Delta r/r$, the outburst profile changes substantially over the small range of $\Delta r_2/r$ in which the instability occurs.

6 DISCUSSION

In this paper we studied a disc instability first explored by Sunyaev & Shakura (1977) and ST93, with a more physically motivated and general formulation of the problem than was used in ST93. In particular, we have improved the description of the disc-field interaction when the disc is truncated outside corotation by deriving conditions for a 'quiescent' state, in which the angular momentum transferred from the star into the disc halts accretion altogether. In agreement with ST93, we observe a wide range of oscillatory behaviour, and the frequency range of individual outbursts spans three orders of magnitude.

The period of the cycle seen in Figs. 3–5 varies from 0.02 to $20t_{\rm c}$, where $t_{\rm c}$ is the nominal viscous time-scale at the corotation radius $t_{\rm c} = r_{\rm c}^2/\nu(r_{\rm c})$. Though cycle times scale with $t_{\rm c}$, this is evidently not the only factor. As discussed in ST93, the viscous time-scale relevant for the cycle period depends on the size of the disc region involved. This depends itself on the cycle period, hence the period must be determined by additional factors. One of these is the mean accretion rate, but the physical conditions in the magnetosphere-disc interaction region have an equally important effect.

From Figs. 7 and 8 it appears that there are two different kinds of instability. One of these operates in a narrow range of accretion rates, around the value where steady accretion would put the inner edge at corotation. The instability in this case is of the type shown in Fig. 3: an approximately sinusoidal modulation, characteristic for a weak form of instability. The inner edge of the disc oscillates about a mean value, but stays inside the width of the transition region. The longer cycles in the upper parts of Figs. 7 and 8 are a strongly non-linear, relaxation type of oscillation. The inner edge is somewhat outside the transition region for much of the cycle with no accretion taking place (the 'quiescent' phase), and dips in for a brief episode of accretion before moving back out again. This is the kind of cycle envisaged by Sunyaev & Shakura (1977). During the quiescent phase, the disc (Sunyaev & Shakura (1977) call it a 'dead disc') extracts angular momentum from the star by the magnetic interaction at its inner edge. These two forms of instability are merged into a continuum in ST93, as a result of the different (and less realistic) assumptions made there about the interaction between disc and magnetosphere outside corotation. This difference also affects the dependence on the mean accretion rate. Whereas in ST93 cyclic behavior was found only in a limited range of accretion rates, our results show that cycles can occur in principle at

arbitrarily low accretion rates, with steadily increasing cycle period and decreasing duty cycle of the accretion phase.

Figs. 4 and 5 show that the radius of the inner edge of the disc does not move by more than 10% around corotation, even at the lowest mean accretion rates. For example in the case $\dot{m}/\dot{m}_{\rm c} = 9.5 \times 10^{-2}$ of Fig. 4, the standard 'ram pressure' estimate would yield a much larger magnetosphere radius, about $r_{\rm m} = 3.6\, r_{\rm c}$. The difference arises because in our cyclic accretion states the conditions in the inner disc are very different from those assumed in conventional estimates of $r_{\rm m}$; the density in the inner disc, for example, is much higher.

At $r_{\rm in} \leqslant 1.1 r_{\rm c}$, the velocity difference between the magnetosphere and the disc is only 5%, much less than the 40% which mass would need in order to escape from the system. 'Propellering' of mass out of the system is thus unlikely to be effective. This does not exclude that some mass loss (powered by a magnetic wind from the disc or the interaction region around the inner edge of the disc) may also take place, but our results show that this is not a necessary consequence for a disc in what is traditionally called 'propeller' regime.

At sufficiently low accretions rates one would expect, however, that propellering would also be a possible outcome: if the rotation rate of the star is high enough, matter could be ejected before it has the time to form a dense disc. The existence of a cyclic form of accretion at low accretion rates thus suggests that two different accretion states are possible, and that there would be a second parameter determining which of the two is realised. This might simply be the history of the system.

If a disc is initially absent and accretion is started, the density will initially be low enough that ejection by propellering can prevent accretion altogether. The cataclysmic variable AE Aqr (e.g. Wynn et al. 1997) is likely to be such a case. On the other hand, if a disc is initially in a high accretion state such that the inner edge is inside corotation, a subsequent decline to low accretion rates could lead to the cyclic accretion described here. Such a situation could be at work in the TTauri star EX Lupi (where the initial high accretion phase has ended). It could also be appropriate for the X-ray millisecond pulsar, SAX J1808.8-3658, which has shown a 1-Hz QPO in the decline phase of several outbursts Patruno et al. (2009). The pile-up of mass at the magnetosphere will maintain the disc this state, and prevent propellering even when the mean accretion rate drops to very low values.

The instability studied in this work has not yet been observed in numerical simulations, partly because most numerical simulations do not run for long enough to observe it, but mainly because most simulations have focused on either accreting or strong propeller cases. However, in virtually all numerical simulations outflows and variability in the disc are observed, with an intensity that varies between different simulations. Gas pile-up at the inner edge of the disc is also observed, with the amount of pile-up tied to the effective diffusivity of magnetic field at the inner edge of the disc (e.g. **?**). The process of closing and opening field lines provides a source of mass to launch both a weakly-collimated outflow (the disc wind) and a well-collimated jet (e.g Hayashi et al. 1996; Goodson et al. 1997; Romanova et al. 2009). The whole cycle takes place on time-scales that can vary between the dynamical and viscous time-scales at the inner edge of the disc, but are generally of higher frequency than the disc instability studied in this paper. The inner edge of the disc also oscillates significantly (although it remains on average outside corotation), from between a few stellar radii (Romanova et al. 2009) up to 30 stellar radii (Goodson et al. 1997). Even if such variability is present, the instability studied in this paper can still occur provided the outflows/accretion bursts generated by field lines opening are not strong enough to fully empty the reservoir of matter accumulating just outside $r_{\rm c}$.

7 CONCLUSIONS

We have studied the accretion of a thin viscous disc on to a magnetosphere of a magnetic star, under the influence of the magnetic torque it exerts on the disc. We focused in particular on cases with low accretion rates. For high accretion rates such that the inner edge $r_{\rm in}$ of the disc is inside the corotation radius, standard steady thin viscous disc solutions are recovered. However, when the inner edge is near corotation we find that the accretion becomes time-dependent, and takes the form of cycles consisting of alternating accreting and non-accreting ('quiescent') states. The period of this cycle varies from a small fraction of the characteristic viscous time scale in the inner disc, $r_{\rm in}^2/\nu$, to a large multiple of it, depending on the mean accretion rate as well as on the precise conditions assumed at the magnetosphere.

These cyclic accretion solutions continue to exist indefinitely with decreasing accretion rate. The cycle period increases, while the duty cycle of the accreting phase decreases with decreasing accretion rate. In the quiescent phase after a burst of accretion, the inner edge of the disc moves outward, and mass starts piling up in the inner regions of the disc. In response, the inner edge eventually starts moving back in again and accretion picks up as $r_{\rm in}$ crosses the corotation radius. This empties the inner regions of the disc, causing the inner edge to move outward again. The cycle thus has the properties of a relaxation oscillator, as found before in ST93. The reservoir involved is the mass in the inner region of the disc. These results (as well as those of Sunyaev & Shakura (1977) and ST93) show that accretion without mass ejection can occur at accretion rates well inside what is usually called the 'propeller' regime. Instead of the mass being ejected, the accreting mass can stay piled up at high surface density in the inner disc, just outside corotation. We have suggested that systems with very low accretion rates can be in either of these states. Propellering would occur when a disc is initially absent and mass transfer is first initiated (the case of AE Aqr for example), while a system with an accretion rate that drops from an initially high value would end in the cyclic accretion state described in this paper. This would apply to most cataclysmic variables and X-ray binaries, as well as some TTauri stars.

8 ACKNOWLEDGMENTS

CD'A would like to thank Stuart Sim for useful scientific discussion, and acknowledges financial support from the National Science and Engineering Research Council of Canada.

REFERENCES

Agapitou V., Papaloizou J. C. B., 2000, MNRAS, 317, 273
Aly J. J., 1985, A&A, 143, 19
Aly J. J., Kuijpers J., 1990, A&A, 227, 473
Blandford R. D., Payne D. G., 1982, MNRAS, 199, 883
Fromang S., Stone J. M., 2009, A&A, 507, 19
Gammie C. F., 1996, ApJ, 457, 355
Ghosh P., Lamb F. K., 1979a, ApJ, 232, 259
Ghosh P., Lamb F. K., 1979b, ApJ, 234, 296
Goodson A. P., Winglee R. M., Boehm K., 1997, ApJ, 489, 199

Hayashi M. R., Shibata K., Matsumoto R., 1996, ApJ, 468, L37+
Herbig G. H., 2007, AJ, 133, 2679
Illarionov A. F., Sunyaev R. A., 1975, A&A, 39, 185
Kulkarni A. K., Romanova M. M., 2008, MNRAS, 386, 673
Lovelace R. V. E., Romanova M. M., Bisnovatyi-Kogan G. S., 1995, MNRAS, 275, 244
Lynden-Bell D., Boily C., 1994, MNRAS, 267, 146
Matt S., Pudritz R. E., 2005, ApJ, 632, L135
Miller K. A., Stone J. M., 1997, ApJ, 489, 890
Paczynski B., 1991, ApJ, 370, 597
Patruno A., Watts A., Klein Wolt M., Wijnands R., van der Klis M., 2009, ApJ, 707, 1296
Popham R., Narayan R., 1991, ApJ, 370, 604
Press W. H., Teukolsky S. A., Vetterling W. T., Flannery B. P., 1992, Numerical recipes in C. The art of scientific computing. Cambridge: University Press 2nd ed.
Pringle J. E., Rees M. J., 1972, A&A, 21, 1
Romanova M. M., Ustyugova G. V., Koldoba A. V., Lovelace R. V. E., 2009, ArXiv e-prints
Shakura N. I., Sunyaev R. A., 1973, A&A, 24, 337
Shu F., Najita J., Ostriker E., Wilkin F., Ruden S., Lizano S., 1994, ApJ, 429, 781
Spruit H. C., Stehle R., Papaloizou J. C. B., 1995, MNRAS, 275, 1223
Spruit H. C., Taam R. E., 1993, ApJ, 402, 593
Sunyaev R. A., Shakura N. I., 1977, Pis ma Astronomicheskii Zhurnal, 3, 262
Ustyugova G. V., Koldoba A. V., Romanova M. M., Lovelace R. V. E., 2006, ApJ, 646, 304
Uzdensky D. A., 2004, Ap&SS, 292, 573
Uzdensky D. A., Königl A., Litwin C., 2002, ApJ, 565, 1191
van Ballegooijen A. A., 1994, Space Science Reviews, 68, 299
Wang Y.-M., 1987, A&A, 183, 257
Wynn G. A., King A. R., Horne K., 1997, MNRAS, 286, 436